

Dopant Distribution between *A* and *B* Sites in the PZT Ceramics of Type ABO_3

P. GONNARD AND M. TROCCAZ

Laboratoire de Génie Electrique et Ferroélectricité, Bâtiment 504, I.N.S.A. de Lyon, 69621 Villeurbanne, France

Received February 17, 1977; in revised form July 13, 1977

The influence of doping oxides on the $PbZr_{0.95}Ti_{0.05}O_3$ composition is studied. A theoretical model allows the doping ion distribution between *A* and *B* sites to be established from its ionic radius. The tolerance factor t , calculated for each doped composition, has a minimum value when the antiferroelectric (AF) property is at its maximum. The experimental results agree well with theoretical calculations.

It is known that the ferroelectric (F) or antiferroelectric (AF) state of a type ABO_3 -perovskite structure is related to its Goldschmidt or tolerance factor t (1):

$$t = \frac{R_A + R_O}{\sqrt{2}(R_B + R_O)},$$

where R_A , R_B , R_O indicate the ionic radius of the large cation, the small cation, and the oxygen ion, respectively. Generally, for a Goldschmidt factor above approximately 0.92, the AF property does not appear. More precise results were obtained while studying the doping effect on a given composition near the F-AF transition phase.

The chosen compound is a lead zirconotitanate $PbZr_{0.95}Ti_{0.05}O_3$ (PZT 95/05) +1 mole% of oxide. In a general way the term dopant is used for atomic percentages less than 5%; above this value, the compound is called a modified PZT.

The conclusions of a recent study (2) where the dopant was supposed to enter either the *A* site or the *B* site are worth special attention:

A dopant which decreases the tolerance factor produces an extension of the AF phase, that is, a temperature increase of the AF → F phase transition. The reverse effect is also observed.

If the doping ion decreases the average volume of the *A* or *B* ions, the unit cell volume is decreased. The reverse effect is also observed.

The extension of the AF phase is caused by the increase of the hydrostatic stress on the *B*-ion sites.

According to the rules of Goldschmidt, the position of the dopant in the *A* or the *B* site can be determined if the ion and the substituted ion radii do not differ by more than 15% (3). These rules cannot be applied for a dopant with an ionic radius very different from R_A and R_B . We propose to evaluate the distribution of a given dopant between two sites in relation to its ionic radius, taking into account the effect on the AF → F transition temperature. Most of the dopants used belong to the rare earth for they present two advantages—their homogeneity and a large range of ionic radii.

I. Ceramic Preparation and Experimental Procedures

1° Material Preparation (4)

The ceramics are made following the standard techniques of sintering. The dopant is added to the base oxides PbO, ZrO₂, TiO₂ in order to facilitate its uniform incorporation into the basic solid solution. The oxides are ball-milled in agate jars with agate balls and ethyl alcohol. The dried mixture is slightly pressed and calcinated in an Al₂O₃ crucible closed with a platinum sheet for 3.5 hr at 950°C, then reground and recalculated. In the crucible a PbO atmosphere is provided by a small platinum container filled with PbO powder. Thus the PbO partial pressure is slightly greater than that of the PZT 95/05 (5). The material is ground for 4 hr, then dried; and collodion is added in order to facilitate pressing. The powder is pressed into small disks and sintered in an Al₂O₃ crucible under a PbO atmosphere, as previously mentioned. The furnace is heated at 200°C/hr to 1300°C, and after a 3-hr soak time the furnace is shut down.

The ceramic is then machined to a thickness of 1 mm and silvered while hot on its two faces. The density of the specimens was at least 95% of theoretical density.

2° Experimental Procedures

The transition temperatures AF → F → P are measured as the temperature rises by recording the dielectric permittivity. These measurements are also made in an electric field of 2000 V/mm. The hysteresis loops at low frequency and the D.T.A. technique are also employed to verify the correctness of the transition temperatures AF → F → P. Specific

resistivity is measured, applying a dc field of 100 V/mm to ceramics, with the help of a Keithley electrometer.

The X-ray examination enables us to measure the unit cell parameter and its variation in relation to the temperature while using a controlled heated chamber. The X-ray equipment used for the powder diffraction is a diffractometer counter using a cobalt $K\alpha_1$ radiation; the measurements are made at large angles (about 74°) starting from the (420) peak. For X-ray examination a ceramic is ground in a mortar, and the powder mixed with paste is spread on a glass substrate. The X-ray diagrams for different temperatures, starting from room temperature, also confirm the F or AF state of the material.

II. Model Used

The ionic radii given by Zeeman (6) (Table I) will be used for the N° 6 coordination ion (in the A site, 12-coordinated, the ionic radius will be multiplied by 1.12).

1° Goldschmidt Factor Calculation

A PZT 95/05 composition doped with 1 mole% of oxide will be considered. In order to write the chemical reaction equations, the site which the doping cation will occupy must be known, as well as the possible positions of the vacancies in site A, B, or O. It can be noted that if the dopant is added to the basic composition, a substitution mechanism occurs during calcination and sintering because of the high volatility of the PbO and because of the reaction taking place in a PbO atmosphere.

An important difficulty encountered is the determination of the vacancies' mean radius. In ionic crystals an elastic relaxation of the

TABLE I

Ion	Pb ²⁺	O ²⁻	Ti ⁴⁺	Zr ⁴⁺	Sc ³⁺	Yb ³⁺	Ho ³⁺	Bi ³⁺	Tb ³⁺	Gd ³⁺	Eu ³⁺	Sm ³⁺	Nd ³⁺	La ³⁺
Ionic radius (Å)	1.32	1.32	0.64	0.87	0.83	0.92	0.95	0.96	0.98	1.00	1.01	1.02	1.06	1.12

lattice around the vacancy occurs. A cationic vacancy behaves like a negative charge and the volume of the vacancy is slightly larger (about 10%) than the ionic volume of the cation. In covalent crystals the relaxation would be negligible (7).

The average cubic radii are calculated with a vacancy radius equal to the ionic radius of the missing ion. In that case the t factor is substantially independent of the distribution of vacancies on the A or B site. The factor t is also nearly independent of the oxygen vacancy radius and slightly modified if the cationic vacancy volume and the cation volume differ by 10%. (See Example).

Example

PZT 95/05 + 1% Tb₂O₃

Undoped PZT 95/05, $t = 0.90720$,

Tb³⁺ at 100% B site (oxygen vacancies)

PbZr_{0.95}Ti_{0.05}O₃ + 0.01 Tb₂O₃ + 0.02 PbO

→ Pb_{1.02}(Zr_{0.95}Ti_{0.05}Tb_{0.02})O_{3.05}□_{0.01},

where □ = vacancy.

$$R_B = \left[\frac{0.95R_{Zr}^3 + 0.05R_{Ti}^3 + 0.02R_{Tb}^3}{1.02} \right]^{1/3},$$

$$R_O = \left[\frac{3.05R_O^3 + 0.01R_{\square}^3}{3.06} \right]^{1/3},$$

$t = 0.90610$ with $R_{\square} = R_O$,

$t = 0.90623$ with $R_{\square} = 0$ (unlikely value).

Tb³⁺ at 50% B site (no vacancy)

$t = 0.90571$,

PbZr_{0.95}Ti_{0.05}O₃ + 0.01 Tb₂O₃

→ Pb₁Tb_{0.01}(Zr_{0.95}Ti_{0.05}Tb_{0.01})O_{3(1+0.01)}.

Tb³⁺ at 100% A site (A -site vacancies)

PbZr_{0.95}Ti_{0.05}O₃ + 0.01 Tb₂O₃

→ Pb_{0.97}Tb_{0.02}□_{0.01}(Zr_{0.95}Ti_{0.05})O₃ +
0.03 PbO,

$t = 0.90531$ with $R_{\square} = R_{Pb}$,

$t = 0.90547$ with $R_{\square}^3 = 1.1 R_{Pb}^3$.

Tb³⁺ at 100% A site (B -site vacancies)

PbZr_{0.95}Ti_{0.05}O₃ + 0.01 Tb₂O₃ → Pb_{0.985}Tb_{0.02}

(Zr_{0.95}Ti_{0.05}□_{0.005})O_{3(1+0.005)} + 0.015 PbO,

$t = 0.90531$ with $R_{\square} = R_B$ for undoped PZT 95/05,

$t = 0.90525$ with $R_{\square}^3 = 1.1 R_B^3$.

According to the firing conditions, B -site

vacancy formation seems more likely than A -site vacancy formation (8).

2° Distribution of the Dopant

The Sc³⁺ ion, which has a smaller radius than the Zr⁴⁺ ion, certainly enters the B site. On the other hand the site occupied by the ions of intermediate ionic radius between those of Pb and Zr is difficult to determine directly. The cell parameter measurements coupled with the tolerance factor calculation can give useful indications.

Figure 1 shows the unit cell volume variations for PZT 95/05 + 1% of oxide in cubic phase.

Let us consider, for example, the PZT 95/05 + 1% Tb₂O₃ composition. The unit cell volume, very near that of the undoped composition, indicates that the Tb³⁺ ion enters neither the 100% B site (the unit cell volume would be greater than that of the undoped product because $R_{Tb} > R_{Zr}$) nor the 100% A site (the unit cell volume would be less than that of the lanthanum-doped PZT because $R_{La} > R_{Tb}$); also, in this last hypothesis the transition temperature $AF_A \rightarrow F_B$ of PZT + 1% Tb₂O₃ would be greater than that of PZT + 1% La₂O₃ since the t factor of the first would be smaller than that of the second; this was not verified experimentally.

In order to clarify the distribution of the dopant between the A and B sites we have calculated the PZT 95/05 t factor with different dopants and as a function of the occupation percentage of the dopant in the B site (Fig. 2).

Let us assume that the doping ion enters the A or B site such that the t -factor value of the doped ceramic is as close as possible to that of the undoped ceramic: in this case all ions would enter the B site, except La and Nd, and the unit cell volumes would increase as a function of ionic radius from Sc to Sm. Such a hypothesis conflicts with the X-ray measurements (Fig. 1).

Assume now that a linear distribution occurs, depending upon the ionic radius (Fig.

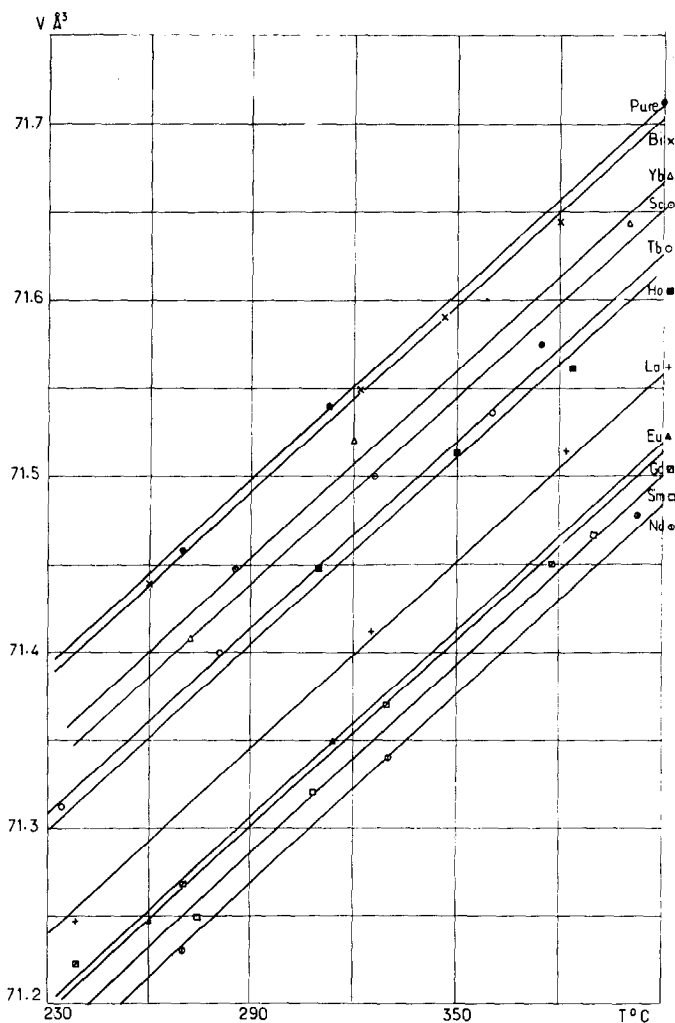


FIG. 1. Unit cell volume variation of doped PZT 95/05 related to temperature.

3). Two reference values are defined taking into account the following considerations:

Figure 2 shows that a critical ionic radius (1.03 Å) gives the same factor t (that is, the same distortion of the cell), whatever the distribution between the A and B sites may be. Consequently we admit that the value $R = 1.03$ Å corresponds to a 50% occupation in the B site (the ion enters the A and B sites equally).

For $t < 1$, the A cation is ferroactive (9), so doping ions larger than the Zr^{4+} ion should enter the B site with difficulty. Thus $R_{Zr^{4+}} =$

0.87 Å corresponds to a 100% occupation in the B site.

The t factor is then calculated for each composition (Fig. 4) taking into account the theoretical distribution between the two sites.

III. Comparison with the Experimental Results

It can be seen in Figs. 4 and 5 (curve a) that the compositions having the smallest t factors (95/05 + 1% Nd_2O_3 , Sm_2O_3 , Eu_2O_3 , La_2O_3) show the greatest AF property since the AF \rightarrow

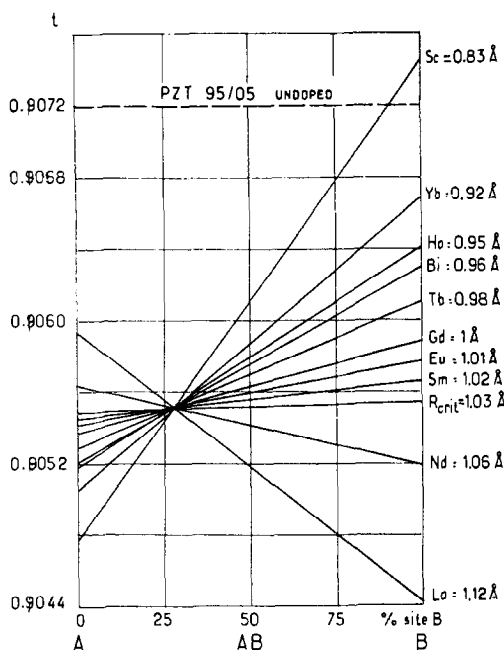


FIG. 2. PZT 95/05 + 1% oxide. Tolerance factor variations related to the doping ion distribution between the A and B sites.

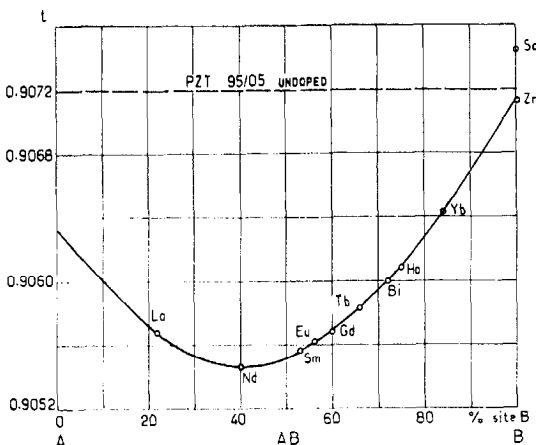


FIG. 4. Tolerance factor calculated from the distribution between the sites given in Fig. 3.

La and Gd dopants, which are assigned the same tolerance factor, present however a small difference between the AF \rightarrow F transition temperatures under 2000 V/mm (respectively 195 and 171°C). This small discrepancy may arise from the inaccurate valuation of vacancy radii or from a deviation with respect to the theoretical model.

F phase transition no longer exists during a temperature rise.

In order to distinguish these aforementioned materials, their AF \rightarrow F transition temperatures under a 2000 V/mm applied electric field (Fig. 5, curve b) are compared. It can be seen that the composition with neodymium still does not exhibit an AF \rightarrow F transition in accordance with its lowest t factor, whereas the other compositions exhibit an induced ferroelectric phase before the paraelectric phase.

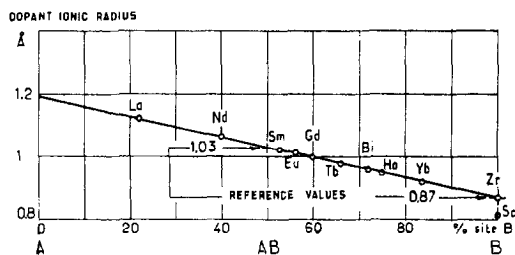


FIG. 3. Theoretical dopant distribution between the A and B sites: PZT 95/05 + 1% oxide.

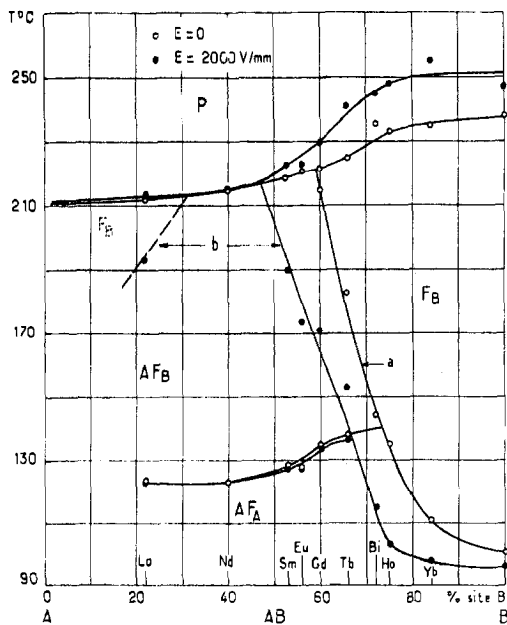


FIG. 5. Phase diagram in a temperature rise experiment (the horizontal axis shows the dopant percentage at the B site): PZT 95/05 + 1% oxide. Curve a: T_{AF-F} zero field; curve b: T_{AF-F} under 2000 V/mm.

TABLE II
PZT 95/05 + 1% L_2O_3

L^{3+}	Color	Grain size (μm)	Resistivity at 278°C ($10^7 \Omega\text{m}$)
La			9
Nd	Light		6.5
Sm		8-15	4.5
Eu			7
Gd	-----		7
Tb		-----	1.6
Ho	Relatively	2-2.5 Inhibited	1.9
Yb	dark	2-2.5 grain growth	0.2
Sc		≤ 1	0.0002

Table II shows that compositions doped with Sc, Yb, Ho, and Tb present some experimental features of the O-position vacancy ceramics (3).

Conclusion

It appears that the change of the AF-F phase transition temperature by a doping oxide is directly related to the cation ionic radius of this oxide and the gradual distribution of this cation between the *A* and *B* sites.

The distribution of an ion on the *A* and *B* sites seems to be a regular function of the ionic radius. A large ionic radius favors the *A* sites.

Experimental measurements by different authors (10, 11) on BaTiO_3 and PbTiO_3 have already shown that a gradual distribution of the cation between sites *A* and *B* was likely.

Our theoretical model predicts and experimental evidence confirms that in a PZT 95/05 composition the strongest stability of the AF phase is obtained with the ion $\text{Nd}^{3+} = 1.06 \text{ \AA}$.

The above study can be applied to all doping oxides with cations of stable valency. We have, for example, verified that a given composition doped with 1% CaO or 0.5% Nd_2O_3 presents a same-phase diagram ($R_{\text{Ca}^{2+}} = R_{\text{Nd}^{3+}} = 1.06 \text{ \AA}$).

PZT 965/035 + 1% CaO

$$T_{\text{AF} \rightarrow \text{F}} = 185^\circ\text{C},$$

$$T_{\text{F} \rightarrow \text{P}} = 228^\circ\text{C},$$

PZT 965/035 + 0.5% Nd_2O_3

$$T_{\text{AF} \rightarrow \text{F}} = 183^\circ\text{C},$$

$$T_{\text{F} \rightarrow \text{P}} = 229^\circ\text{C}.$$

These and previous results (2) indicate that the radius of the cation dominates the AF \rightarrow F phase stability over the effects of charge, polarizability, and vacancies that must be introduced.

References

1. N. VENEVTSEV AND G. S. ZHDANOV, *Bull Acad. Sci. URSS Ser. Phys.* **20**, 161 (1956).
2. M. TROCCAZ, P. GONNARD, Y. FETIVEAU, L. EYRAUD, AND G. GRANGE, *Ferroelectrics* **14**, 679-682 (1976).
3. B. JAFFE, W. R. COOK, AND H. JAFFE, "Piezoelectric Ceramics", Academic Press, New York (1971).
4. M. TROCCAZ, Thèse Lyon, n° 1-75-005 (1975).
5. K. H. HARDTL AND H. RAU, *Solid State Commun.* **7**, 41-45 (1969).
6. J. ZEEMAN, "Chimie Cristalline," Dunod, Paris (1970).
7. Y. ADDA AND J. PHILIBERT, "La diffusion dans les solides," Vol. 1, B.S.T.N., Presses Univ. of France, Paris (1966).
8. D. HENNINGS AND K. H. HAERDTL, *Phys. Status Solidi A* **3**, 465-474 (1970).
9. R. V. KOLESOVA, E. G. FESENKO AND V. P. SAKHNENKO, *Sov. Phys.* **16**, 301-304 (1971).
10. T. MURAKAMI, T. MIYASHITA, M. NAKAHARA AND E. SEKINE, *J. Amer. Ceram. Soc.* **56**, 294-97 (1973).
11. D. HENNINGS AND H. POMPLUN, *J. Amer. Ceram. Soc.* **57**, 527-30 (1974).